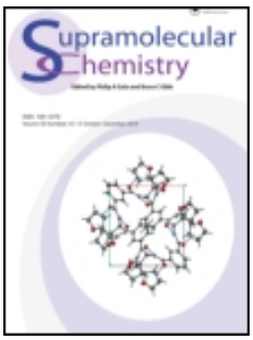

Supramolecular Chemistry

ISSN: 1061-0278 (Print) 1029-0478 (Online) Journal homepage: http://www.tandfonline.com/loi/gsch20

Seven-coordinated cobalt(II) complexes with 2,6-diacetylpyridine bis(4-hydroxybenzoylhydrazone): synthesis, characterisation, DNA binding and cleavage properties

Ramazan Gup, Cansu Gökçe & Nefise Dilek

To cite this article: Ramazan Gup, Cansu Gökçe & Nefise Dilek (2015) Seven-coordinated cobalt(II) complexes with 2,6-diacetylpyridine bis(4-hydroxybenzoylhydrazone): synthesis, characterisation, DNA binding and cleavage properties, Supramolecular Chemistry, 27:10, 629-641, DOI: 10.1080/10610278.2015.1051978

To link to this article: http://dx.doi.org/10.1080/10610278.2015.1051978

View supplementary material

Published online: 24 Jun 2015.

Submit your article to this journal

Article views: 82

View related articles

View Crossmark data

Full Terms & Conditions of access and use can be found at
http://www.tandfonline.com/action/journalInformation?journalCode=gsch20

Download by: [University of Nebraska, Lincoln] **Date:** 20 October 2015, At: 19:53

Supramolecular Chemistry, 2015
Vol. 27, No. 10, 629–641, http://dx.doi.org/10.1080/10610278.2015.1051978

Taylor & Francis
Taylor & Francis Group

Seven-coordinated cobalt(II) complexes with 2,6-diacetylpyridine bis(4-hydroxybenzoylhydrazone): synthesis, characterisation, DNA binding and cleavage properties

Ramazan Gup[a]*, Cansu Gökçe[a] and Nefise Dilek[b]

[a]*Department of Chemistry, Faculty of Science, Mugla Sıtkı Koçman University, 48100 Mugla, Turkey;* [b]*Department of Physics, Faculty of Arts and Sciences, Aksaray University, 68100 Aksaray, Turkey*

(*Received 26 April 2015; accepted 13 May 2015*)

Synthesis and characterisation of three seven-coordinated cobalt(II) complexes of 2,6-diacetylpyridine bis(4-hydroxybenzoylhydrazone) (H_4L) ligand, $[Co(H_2L)(H_2O)_2]$ **(1)**, $[Co(H_4L)(N_3)_2]$ **(2)** and $[Co(H_4L)(NCS)_2]$ **(3)** are described. The structures of the complexes were characterised by elemental analysis, IR, UV–vis and magnetic susceptibility measurement. The molecular structure of the $[Co(H_4L)(NCS)_2]$ **(3)** was also determined by X-ray crystallography. Single crystal X-ray revealed that the Co(II) complex **(3)** has a pentagonal–bipyramidal coordination geometry, with pentadentate N_3O_2 ligand in the equatorial plane of the bipyramid and two isothiocyanato groups in the axial area. Interaction of the cobalt(II) complexes with CT-DNA was investigated by absorption titration method and viscosity measurements. Cleavage activity of the complexes with pBR 322 plasmid DNA was evaluated by agarose gel electrophoresis in presence and absence of an oxidative agent, and the mechanism of DNA cleavage was investigated. The results suggest that the cobalt(II) complexes bind effectively and they exhibit nuclease activity, which has strong dependence on the concentration of complex and reaction time, both in presence and absence of hydrogen peroxide.

Keywords: 2,6-diacetylpyridine, aroylhydrazone; cobalt(II) complex; DNA binding; nuclease activity

Supramolecular Chemistry 2015.27:629-641.

1. Introduction

DNA is the essential target molecule for most disease therapies such as anticancer and antiviral. Any disorder in gene expression may cause diseases and plays a secondary role in the outcome and severity of human diseases. The interaction of transition metal complexes with DNA has been intensively studied to design of new types of pharmaceutical compounds. The metal complexes interact with DNA and induce the breakage of DNA strands by appropriate methods (*1–6*). Thus, there is an increasing focus on the binding study of small molecules to DNA during the last decades. A more complete understanding of DNA binding is necessary to design a new drug.

Cobalt is transition metal generally regarded as nutritionally essential microelement for humans. Cobalt (II) is classified as 'borderline' between 'hard' (a-class) and 'soft' (b-class) metals regarding their metal–DNA interactions as they show more affinity for both the heterocyclic bases and the phosphate group of DNA; therefore, the interaction of cobalt complex with DNA has attracted much attention (*7–10*). Apart from being an essential element, it may be less toxic yet cobalt(II) ions are toxic at higher concentration. The biological role of cobalt is mainly focused on its presence in the active centre of vitamin B12, which regulates indirectly the synthesis of DNA (*11*). Cobalt acts as catalyst in a variety of enzyme system functions and in coenzymes in several biochemical processes. Numerous cobalt complexes showing antitumor, antiproliferative, antimicrobial, antifungal, antiviral and antioxidant activities have been reported (*12–23*).

Geometry of the coordination compounds which depends on the metal ion type and different functional groups in the ligands is primarily responsible for the affinity of the metal complexes to DNA. Transition metal complexes with tunable coordination environments offer a great scope for the design of species that are suitable for DNA binding and cleavage activities. Therefore, the investigation on the interaction of the Schiff base transition metal complexes with DNA has a great significance for disease defense, new medicine design and clinical application of drugs.

Many cobalt complexes with different geometries have been synthesised, characterised and their interactions with DNA have been studied extensively. On the other hand, many heptacoordinate metal complexes based on bis (acylhydrazone) ligands have been synthesised and characterised (*24–29*), yet only a few of them have reported on their pharmacological properties and RNA interactions. We have initiated the synthesis, characterisation and investigation of DNA interaction of heptacoordinated Co(II) complexes derived from 2,6-diacetylpyridine bis(4-aroylhydrazone) (*25*). In continuation of our studies, we report herein the synthesis, characterisation and DNA binding and cleavage activities of three new seven-

*Corresponding author. Email: rgup@mu.edu.tr

© 2015 Taylor & Francis

coordinated Co(II) complexes of a pentadentate bis (aroylhydrazone) ligand.

2. Results and discussion

2.1 IR spectroscopy

In the IR spectra of the $[Co(H_2L)(H_2O)_2]$ complex, the amide I band disappears and a new band is observed at 1590 cm^{-1} probably due to ⟩C═N—N═C⟨ stretching vibration indicating transformation of the carbonyl group to its enolic form through keto-enol tautomerism and subsequent coordination of the enolic oxygen to cobalt(II) ion after deprotonation (*30–33*). The IR spectra of $[Co(H_4L)(NCS)_2]$ and $[Co(H_4L)(N_3)_2]$ show strong stretching vibrations peaks at 1645 and 1590 cm^{-1}, 1649 and 1598 cm^{-1} due to carbonyl and imine groups, respectively, indicating the coordination in the keto form. The azido complex exhibits two strong peaks at w 2042 cm^{-1} and w 1277 cm^{-1}. These peaks are attributed to ν_a and ν_s of the coordinated azido group. The IR spectrum of the complex $[Co(H_4L)(NCS)_2]$ has two additional bands at 2089 cm^{-1} and 920 cm^{-1} corresponding to CN and CS modes of the coordinated NCS group, respectively. The position of these bands may be indicated by the coordination of NCS group through the nitrogen atom (*34–37*). The stretching vibration of phenolic OH group remains almost unaltered, suggesting non-involvement of this group in the complex formation. The amide NH stretching band is not observed in the IR spectra probably due to overlapping with the broad OH stretching frequency.

On the basis of IR spectral data, we can conclude that in the case of the complex **1**, the acylhydrazone (H_4L) acts as a di anionic O,N,N′,N,O-pentate ligand and the sixth and seventh positions are occupied by two water molecules. On the other hand, the H_4L acts as a neutral O,N,N′,N,O-pentate ligand and the axial positions are occupied by SCN^- or N_3^- anions with pentagonal–bipyramidal geometry in the complexes **2** and **3**.

2.2 Electronic absorption spectra

The cobalt(II) complexes exhibit two intense bands at 268 nm and around 352 nm and a shoulder around at 432 nm. The first band is assignable to the aromatic ring transition $\pi \rightarrow \pi^*$. The second intense band can be assigned the $n \rightarrow \pi^*$ type electronic transitions. The week shoulder observed in the visible region is also probably due to allowed charge-transfer transition.

For the complexes **1**, **2** and **3**, room temperature magnetic moments values are 4.25 and 4.27 B.M., respectively. These μ_{eff} values lie in the range corresponding to three unpaired electrons for pentagonal bipyramidal geometry ($S = 3/2$) around cobalt(II), d^7 complexes.

2.3 Description of crystal structure of $[Co(H_4L)(SCN)_2]$ (3)

The crystal structure is shown in Figure 1 with atom-numbering scheme. Basic crystal data, description of the diffraction experiment and details of the structure refinement are given in Table 1. Selected bond distances and angels are presented in Table 2. The cobalt(II) complex **3** crystallises in the monoclinic *C*2/*c* space group and has a crystallographic symmetry of two-fold axis. In the asymmetric unit, there are two DMF (dimethylformamide) molecules. The central Co(II) atom is seven-coordinated with N_5O_2 coordination environment and has a pentagonal bipyramid coordination geometry. The 2,6-diacetylpyridine bis(4-hydroxybenzoyl hydrazone) acts as a pentadentate neutral ligand which is bound to the Co(II) ion through three nitrogen atoms [N(2), N(2^i) and N(3)] and two oxygen atoms [O(2) and O(2^i)] defining the equatorial coordination plane. The pentagonal–bipyramidal coordination geometry around cobalt atom is completed by two NCS groups which are bound to Co(II) in axial positions. The two Co—N bonds in axial position are significantly shorter (2.089 Å) than the three Co—N bonds in the pentagon (2.237 and 2.197 Å). The large difference in the Co—N bond lengths in the equatorial and axial positions cannot be explained since the high spin Co(II) ion in the pentagonal bipyramid crystal field is not be expected a Jahn-Teller distortion. On the other hand, a similar difference in such bond lengths is seen in the other 2,6-diacetylpyridine bis(aroylhydrazone) mangan(II) complex (*35*) having a pentagonal bipyramidal geometry with two isothiocyanato groups in the axial position.

In the structures of the Co(II) complex, O2—Co—$O2^i$ bond angle is remarkably larger than the other four angles in the equatorial plane. The central angle of a regular pentagon is 72°, whereas the O2—Co—$O2^i$ angle in the titled Co(II) complex is 80.14(8)°. In contrast, the N3—Co—N2($N2^i$) and O2—Co—N2 ($O2^i$—Co—$N2^i$) angles are 69.92(5)° and 70.02(6)°, respectively. On the other hand, the regular angle between axial and equatorial positions is 90° while the observed N4—Co—N3, N4—Co—O2, N4—Co—N2 and $N4^i$—Co—N2 angles are 92.38(6), 88.85(8), 92.97(8) and 88.66(8), respectively. The bond angle of the N4—Co—$N4^i$ in the axial position is 175.3(1)°. These observations indicate that the complex has a slightly distorted pentagonal bipyramid geometry around cobalt(II). In the complex (**3**), the C8—N2 and C7—O2 bonds are 1.280 and 1.231 Å, respectively, indicating that they are double bonds. C3—O1 single bond length is 1.349 Å. The all chelate rings of molecule are essentially planar. The other bond lengths and angles in the molecule are within expected ranges, and similar to the other studies (*38*, *39*).

The H atoms were positioned geometrically, with C—H = 0.93 Å (aromatic), N—H = 0.86 Å and

Supramolecular Chemistry 2015.27:629-641.

Supramolecular Chemistry 2015.27:629-641.

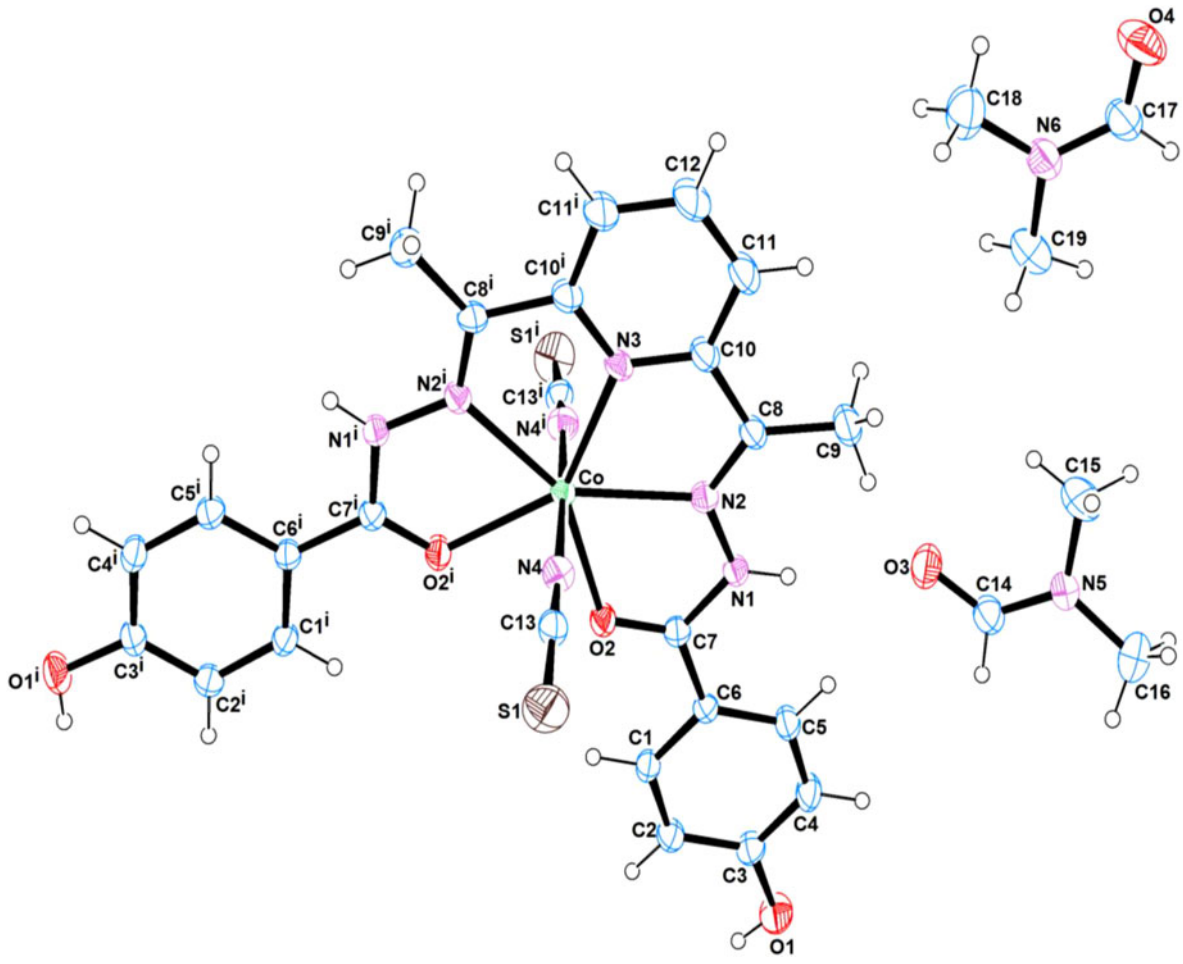

Figure 1. (Colour online) An ORTEP drawing of molecular structure with the crystallographic numbering scheme. Thermal ellipsoids are drawn at 30% probability levels.

O—H = 0.82 Å, and constrained to ride on their parent atoms, with U_{iso} (H) = 1.2U_{eq} (C,N) and U_{iso} (H) = 1.5U_{eq} (O) Also, the methyl H-atoms were positioned geometrically, with C—H = 0.96 Å and constrained to ride on their parent atoms with U_{iso} (H) = 1.5U_{eq} (C).

As can be seen from the packing diagram (Figure 2), inter-molecular N—H···O, O—H···O hydrogen bonds and C—H···π hydrogen bonds (Table S2) link the molecules and these hydrogen bonds may be effective in the stabilisation of the crystal structure. In these interactions, the O3 and O4 atoms act as acceptors, and both of the DMF molecules form hydrogen bonds with the basic molecule.

2.4 Thermal analyses

According to TGA curves (Figures S1, S2 and S3), in the first step of decomposition, the titled cobalt(II) complexes show weight loss of 8.00 (calculated 7.74%) below 200°C for **1**, 15.00% (calculated 14.63%) and 18.60% (calculated 19.14%) below 300°C for **2** and **3**, respectively. These weight losses correspond to two moles of monodentate ligands occupying the axial position of the pentagonal bipyramidal cobalt(II) complexes; two moles of water for **2**, two moles of N_3^- for **2** and two moles of SCN^- for **3**. The other steps of decomposition of these cobalt(II) complexes appeared above 300°C involve the removal of the organic part of ligand leaving cobalt oxide as a residue.

2.5 Binding studies

2.5.1 Absorption spectral titrations

Absorption titration is an effective method to examine the binding mode of DNA with metal complexes (40–42). Usually, when a drug interacts with DNA and forms a new complex, change in the UV–vis absorption spectra of the drug occurs. Particularly, hypochromism with usually with a red shift due to strong stacking interactions between aromatic chromophore of molecule and the base pairs of

Table 1. Crystallographic data and structural refinement for the cobalt(II) complex.

Chemical formula	$Co[C_{25}H_{21}N_7O_4S_2]\cdot 2(C_3H_7NO)$
Formula weight (amu)	898.92
Crystal form, colour	Prism, orange
Crystal size (mm)	$0.670 \times 0.320 \times 0.270$
Crystal system	Monoclinic
Space group	*C*2/*c*
a (Å)	13.603(1)
b (Å)	17.627(2)
c (Å)	19.594(2)
α (°)	90.00
β (°)	108.833(4)
γ (°)	90.00
V (Å^3)	4446.5(7)
Z	4
D_x (g/cm^3)	1.343
λ (MoK_α) Å	0.71073
μ(MoK_α) mm^{-1}	0.540
T (K)	296(2)
θ_{max}	28.15
θ_{min}	2.24
H	−16–16
K	−22–22
L	−24–24
Number of reflections measured	50025
Number of independent reflections	4545
Number of reflections [$I > 2\sigma(I)$]	3996
Number of parameters	275
R	0.0448
Rw	0.1437
S	1.069
Weighting scheme	$1/[\sigma^2 (F_o^2) + (0.1040P)^2$ $P = (F_o^{2+}2F_c^2)/3$
$(\Delta/\sigma)_{max}$	1.277
$(\Delta\rho)_{max}$, $(\Delta\rho)_{min}$ (e Å^{-3})	0.070, −0.420
Measurements	Bruker APEXII
Structure determination	Direct method (SHELXS-97)
Refinement	Full matrix l.s. (SHELXL-2013)
Treatment of hydrogen atoms	Geometric calculation

DNA may appear in the case of an intercalative binding mode. On the other hand, the absorption intensities of drugs are increased (hyperchromism) upon increasing the concentration of CT-DNA due to a damage of the CT-DNA double-helix structure. The extent of the hyperchromism is indicative of the partial or non-intercalative binding modes, such as electrostatic forces, Vander Waals interaction, hydrogen bonds and hydrophobic interaction.

The electronic absorption spectra of the cobalt(II) complexes in the absence and in the increasing concentrations of CT-DNA are given in Figure 3(A)–(C). Upon addition of DNA, interesting changes in the absorption spectra of the cobalt(II) complexes are observed. The bands at 352 and 354 nm for the titled Co (II) complexes exhibit hypochromism together with a considerable blue shift (~25 nm). With increasing concentration of DNA, these absorptions of the complexes almost disappeared and a new band appears at ~327 nm. These spectral changes afforded an isobestic point at 333.5 nm for (**1**), 331.5 nm for **2** and 330.5 nm for **3** which indicates the existence of the single binding mode. To the best of our knowledge, there are a few literatures related to Cu(II), Zn(II) and Pt(II) complexes *(43–45)* where such type of spectral changes have been observed and they have described covalent binding of metal complexes with DNA. On the other hand, we have not found any cobalt(II) report exhibiting such type of spectral changes. Keeping these observation in mind, we indicate that it is possible that with increasing concentration of DNA, when more binding sites are available, the titled cobalt(II) complexes are bounded to the nucleic acid base such as guanine (N7) and a new complex is generated during DNA interaction. The changes in the UV–vis spectra of the cobalt(II) complexes suggest that that the binding natures of the titled Co(II) complexes with DNA are very similar, whereas the absorption spectra of the cobalt(II) complexes are significantly changed upon addition of DNA, suggesting that the architectures of the complexes are modified by binding.

In order to see whether the DNA coordinates to cobalt complexes, we performed the reverse titration experiments for the complex **3** (Figure 4). The increasing concentrations of the cobalt(II) complex were added into DNA solution in this titration experiment. The spectra of the complex were not seen initially until ~15 μM, yet further addition of the complex afforded the spectra of **3**. On the other hand, this spectrum exhibited significant differences from DNA-free spectrum of the complex **3**. For instance, the peak observed at 352 nm in the spectra underwent a slight blue shift to 350 nm while a new shoulder at ~326.5 nm in the DNA-free spectra of **3** in reverse titration with DNA. These observation may indicate the formation of new species consist of CT-DNA and the cobalt(II) complex. Covalent binding involves the coordination of the nitrogenous base or the phosphate moiety of the DNA to the central metal atom. The complexes where the metal is coordinatively unsaturated or is coordinated to substitutionally label ligands are suitable for the covalent bonding. Each of the cobalt(II) complexes synthesised in our study has two monodentated label ligands such as H_2O, N_3^- or NCS^- in the axial positions. Therefore, it is reasonably expected that one of the these label ligands can split from the pentagonal–bipyramidal complex and the DNA can coordinate the cobalt(II) ions of the unsaturated complex formed during the interaction of the cobalt(II) complex with DNA.

The binding constant, K_b, was determined from the plot of [DNA]/($\varepsilon_a - \varepsilon_f$) versus [DNA] (Table 3). The binding constant values of 5.00×10^3 M^{-1} for **1**, 3.0

Supramolecular Chemistry 2015.27:629-641.

Table 2. Selected bond lengths (Å), bond angles (°) and torsion angles (°) of the cobalt(II) complex.

Bond lengths		Bond angles				Torsion angles	
Co—N4	2.089(2)	N4—Co—N4$^{\#}$	175.3(1)	N4—Co—N2$^{\#}$	88.66(8)	C7—N1—N2—C8	179.8(2)
Co—N3	2.197(3)	N2—Co—N2$^{\#}$	139.8(1)	N4$^{\#}$ —Co—N2$^{\#}$	92.97(8)	C7—N1—N2—Co	− 3.4(2)
Co—O2	2.218(2)	O2$^{\#}$ —Co—O2	80.14(8)	N2—N1—C7	114.6(2)	C1—C2—C3—O1	178.3(3)
Co—N2	2.237(2)	N4—Co—N3	92.38(6)	C8—N2—N1	121.7(2)	Co—O2—C7—N1	3.9(3)
S1—C13	1.633(3)	N4$^{\#}$ —Co—N3	92.38(6)	C8—N2—Co	122.2(2)	Co—O2—C7—C6	− 175.7(2)
N1—N2	1.366(3)	N4—Co—O2$^{\#}$	87.52(8)	N1—N2—Co	116.0(1)	C1—C6—C7—O2	2.2(3)
N2—C8	1.280(3)	N4$^{\#}$ —Co—O2$^{\#}$	88.85(8)	C10$^{\#}$ —N3—C10	119.7(3)	C5—C6—C7—O2	− 179.0(2)
N3—C10	1.337(3)	N4—Co—O2	88.85(8)	C10$^{\#}$ —N3—Co	120.1(1)	N1—N2—C8—C10	177.9(2)
N4—C13	1.144(4)	N4$^{\#}$ —Co—O2	87.52(8)	C10—N3—Co	120.1(1)	Co—N2—C8—C10	1.3(3)
O1—C3	1.349(3)	N3—Co—O2$^{\#}$	139.93(4)	C13—N4—Co	173.7(2)	N1—N2—C8—C9	− 0.1(4)
O2—C7	1.231(3)	N3—Co—O2	139.93(4)	C7—O2—Co	119.3(1)	Co—N2—C8—C9	− 176.7(2)
		N4—Co—N2	92.97(8)	O2—C7—N1	119.8(2)	Co—N3—C10—C11	− 179.9(2)
		N4$^{\#}$ —Co—N2	88.66(8)	N4—C13—S1	179.6(3)	Co—N3—C10—C8	1.9(3)
		N3—Co—N2	69.92(5)			N2—C8—C10—N3	− 2.0(3)
		N3—Co—N2$^{\#}$	69.92(5)			C9—C8—C10—N3	176.2(2)
		O2$^{\#}$ —Co—N2	150.13(7)			O3—C14—N5—C15	2.2(6)
		O2—Co—N2	70.02(6)			O3—C14—N5—C16	177.9(4)
		O2$^{\#}$ —Co—N2$^{\#}$	70.02(6)			O4—C17—N6—C19	− 175.2(3)
		O2—Co—N2$^{\#}$	150.13(7)			O4—C17—N6—C18	2.7(5)

Note: Symmetry transformations: $^{\#}$ $-x, y, -z + 1/2$.

Supramolecular Chemistry 2015.27:629-641.

$\times 10^3\,M^{-1}$ for **2** and $4.50 \times 10^3\,M^{-1}$ for **3** suggest that the complex **1** has slight higher affinity to DNA than those of the other cobalt(II) complexes. However, these observations are smaller than those of previously reported cobalt (II) complexes (*3*, *4*, *7*, *25*).

2.5.2 *Viscosity measurements*

The binding modes of the cobalt(II) complexes to DNA are further confirmed via viscosity measurement carried out by keeping DNA at 0.5 mM and varying the concentrations of Co(II) complexes, 4,6-diamidino-2-phenylindole (DAPI) or EB. The results are shown in Figures 5, S4 and S5 for the complexes **3**, **1** and **2**, respectively. A classical intercalation mode requires that the DNA helix lengthens as base pairs are separated to accommodate the binding ligand, and thus leading to an increase in the viscosity of a DNA solution. In contrast, a partial or nonclassical intercalation of ligand could bend (or kink) DNA helix, resulting in the decrease of its effective length and its viscosity or having a smaller effect on viscosity (*46–48*). In this study, we have used the ethidium bromide (EB) and DAPI as references. As can be seen from Figure 5, EB, being a well-known DNA intercalator between DNA base pairs and thus lengthening the DNA double helix, increases the relative viscosity of DNA sharply, whereas the viscosity of double strand DNA remains almost unchanged in the case of DAPI, minor groove binding agent. Here, the relative viscosity of DNA solutions increases upon increasing the amounts of cobalt (II) complexes, indicating that all three cobalt(II) complexes could bind to DNA not only by covalent interaction but by the classical intercalation binding mode, and this is also in agreement with the result of absorption spectra. This situation may be related to the molecular structures of the cobalt(II) complexes. The cobalt(II) complexes have been proposed to have slightly distorted pentagonal bipyramidal geometries. The pyridine ring and two aroylhydrazone groups are in the same plane. Therefore, due to having a planar geometry, the cobalt (II) complexes easily penetrate into DNA base pairs and bind to DNA probably through a stacking interaction between the aromatic chromophore of the cobalt(II) complexes and the base pairs of DNA.

2.6 *Nuclease activity of the cobalt(II) complexes*

The oxidative and hydrolytic DNA cleaving abilities of the cobalt(II) complexes have been examined by the agarose gel electrophoresis pattern of pBR 322 plasmid DNA at 37°C in TBE buffer (*25*, *49–51*). DNA cleavage reaction was monitored by relation of supercoiled circular pBR 322 (Form I) into nicked circular Form II and linear Form III. If only one DNA strand is cleaved, the Form I will relax to produce a nicked circular from. If both strands are cleaved, then form III will be produced. These three plasmid DNA conformations are distinguishable when subjected to agarose gel electrophoresis since a relatively fast migration is observed for supercoiled form when the plasmid DNA is subjected to electrophoresis. The nicked circular form migrates slowly and the linear form migrates between Form I and Form II.

The titled cobalt(II) complexes exhibit effective cleavage activity converting the supercoiled DNA into the open circular and linear forms in the presence and absence of hydrogen peroxide. The cleavage reactions

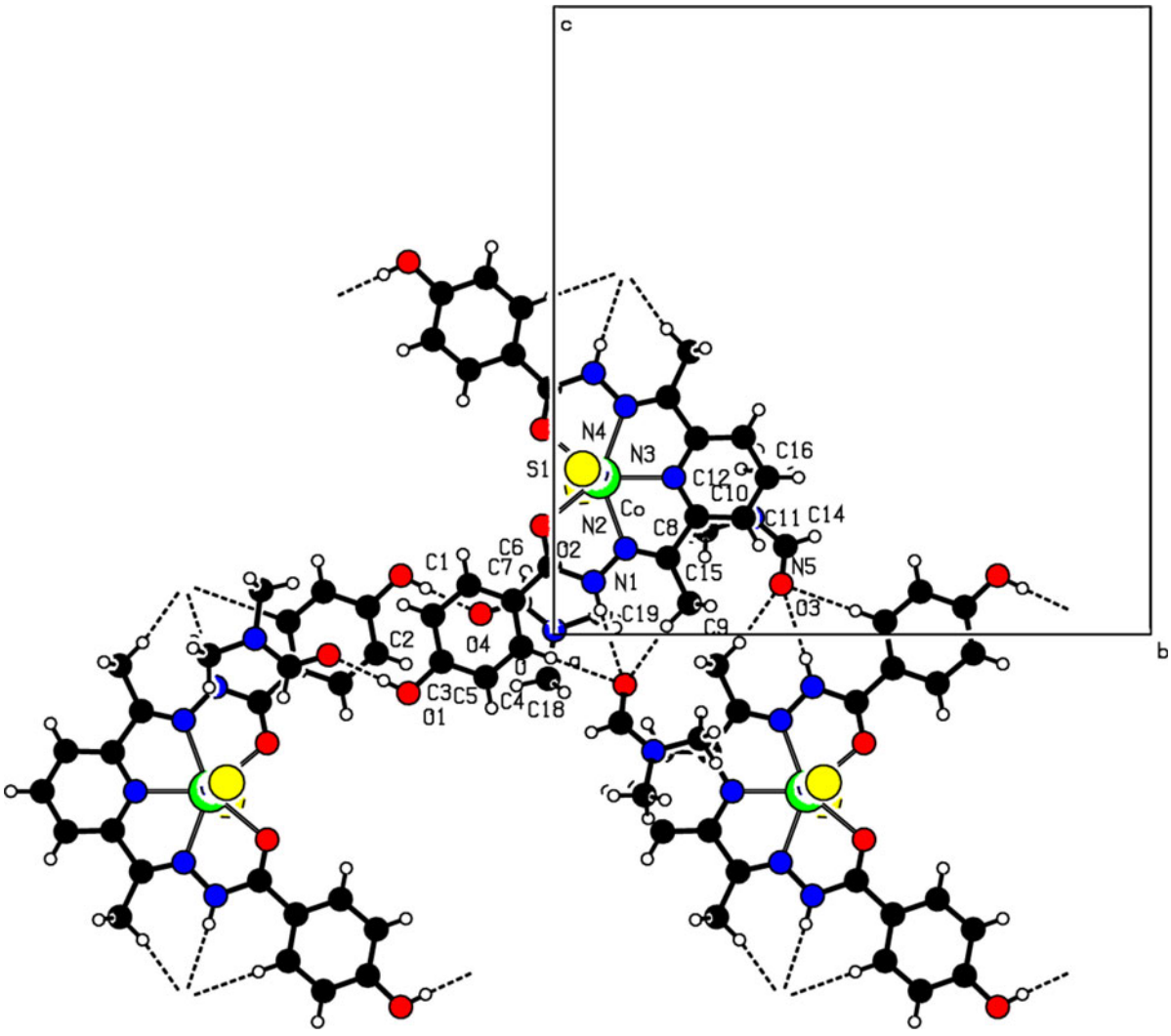

Figure 2. (Colour online) A packing diagram for molecule, projected along (a) direction. Hydrogen bonds are indicated by dashed lines.

meditated by the titled complex were performed under different concentrations of complex (25–200 μM) and incubation time (0.5–6 h) at 37°C. All the results indicate that the oxidative and hydrolytic DNA cleavage properties of the complex are obviously both concentration and incubation time-dependent.

Figure 6 shows the electrophoresis results of the DNA cleavage induced by the increasing concentration of the titled cobalt(II) complexes in the presence of hydrogen peroxide on 3-h incubation at 37°C. DNA cleavage abilities of the cobalt(II) complexes **1** and **3** are almost similar between 25 and 200 μM. Both complexes convert the supercoiled DNA to nicked and linear forms at all concentrations, yet form I DNA is still observed at all concentrations (Figure 6(A),(C), lanes 2–6). The cleavage percentage of nicked form is much higher than that of linear form for both complexes. On the other hand, the cobalt(II) complex **2** exhibits little different DNA cleavage affinity from the cobalt(II) complexes **1** and **3** in these concentrations. It converts slightly the supercoiled DNA only to nicked form at 25 μM (Figure 6(C), lane 5). At the higher concentration of **2** (≥50 μM), both forms II and III are observed besides form I. The percentages of forms II and III DNA scale up with increasing concentrations of the all three cobalt(II) complexes.

In order to obtain information about the active chemical species effecting DNA damage, the comparative oxidative DNA cleavage reactions were also carried out in the presence of various radical scavengers (Figure 7), such as superoxide dismutase as superoxide anion radicals ($O_2^{\cdot-}$), catalase as a hydrogen peroxide scavenger, NaN_3 as $^1O_2$ scavenger, and DMSO and KI as $OH^{\cdot}$ radical scavengers. As shown in Figure 7, the hydrogen peroxide scavenger catalase significantly inhibits the cleavage activity of all three cobalt(II) complexes (lane 6) suggesting that hydrogen peroxide is involved in the

Supramolecular Chemistry 2015.27:629-641.

Supramolecular Chemistry 2015.27:629-641.

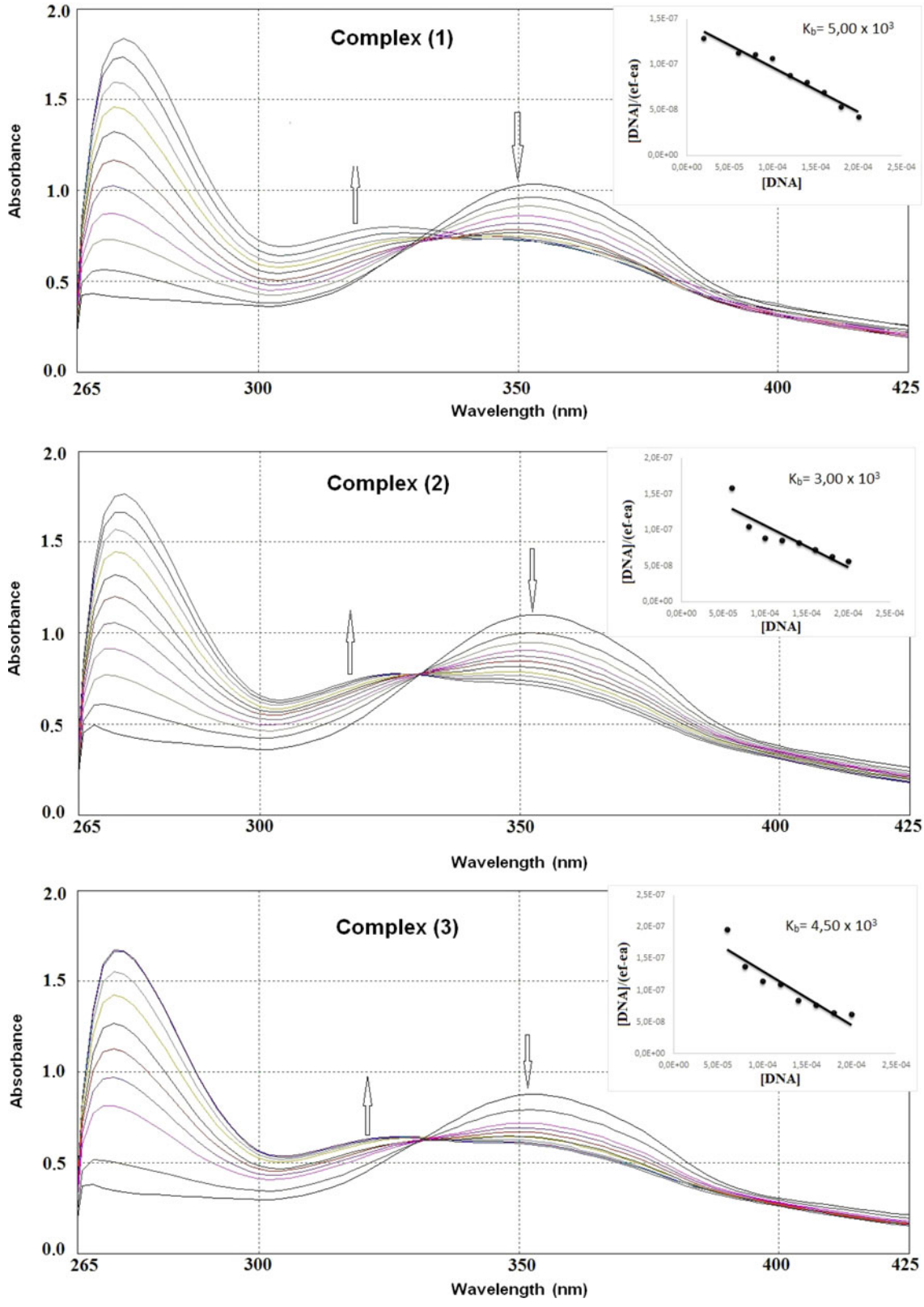

Figure 3. (Colour online) Absorption spectra of the cobalt(II) complexes with increasing concentration of CT-DNA. [Complex] = 25 μM, [DNA] = 0–50 μM.

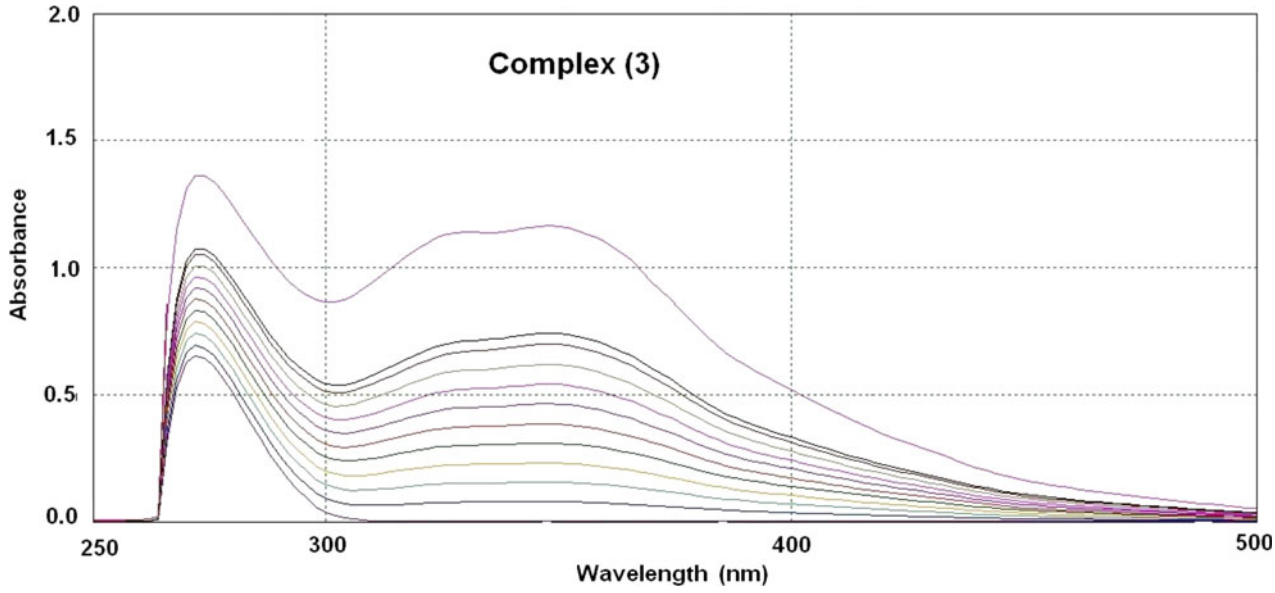

Figure 4. (Colour online) Absorption spectra of the CT DNA with increasing concentration of cobalt(II) complex **3**. [DNA] = 20 μM, [Complex] = 2.5–40 μM.

Table 3. Effect of CT-DNA on the absorbance bands and binding constant of the complexes and adducts.

	λ_{max} (nm)				
Complex	Free	Bound	Δλ (nm)	H (%)	K_b (M^{-1})
$[Co(H_2L)(H_2O)_2]$ (**1**)	352.0	326.0	26.0	28.12	5.00×10^3
$[Co(H_4L)(N_3)_2]$ (**2**)	352.0	328.0	24.0	27.40	4.50×10^3
$[Co(H_4L)(SCN)_2]$ (**3**)	354.0	326.0	24.0	26.23	3.00×10^3

cleavage reaction of complex **1**. Further, addition of singlet-oxygen scavenger NaN_3 results in the inhibition of cleavage activity, as shown in Figure 7, lane 5, indicating that the singlet-oxygen radical is responsible for the nuclease activity exhibited the complex **1** to some extent. On the other hand, the nuclease activities of the cobalt complexes are not inhibited in the presence of the other scavengers employed in this study. It may be concluded from these results that the complex **1** may cleavage the DNA probably through oxidative mechanism, whereas the

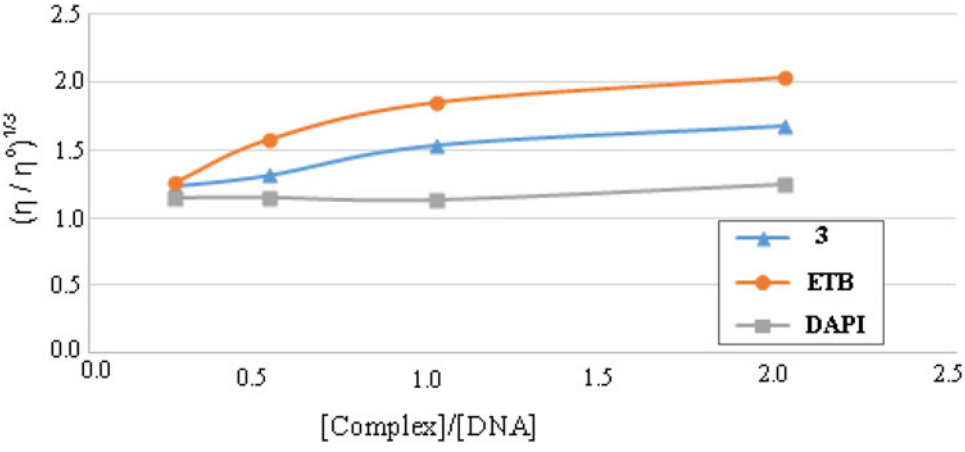

Figure 5. (Colour online) Effect of increasing amounts of the cobalt(II) complex (3), DAPI and EB on the relative viscosity of calf thymus DNA at room temperature.

Supramolecular Chemistry 2015.27:629-641.

Supramolecular Chemistry 2015.27:629-641.

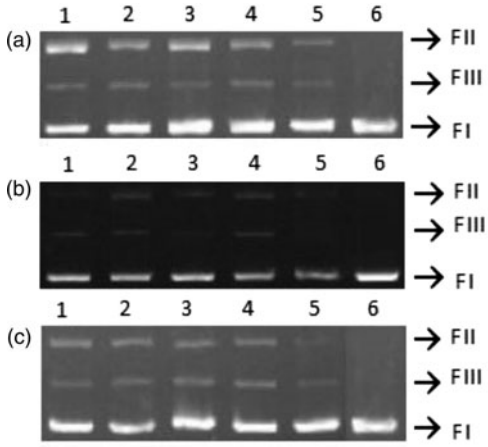

Figure 6. Agarose gel electrophoresis patterns of plasmid pBR 322 DNA after 3 h incubation with various concentrations of the cobalt(II) complexes **1** (a), **2** (b), **3** (c) in the presence of H_2O_2. Lane 1, $[Co(H_4L)(X)_2]$ (200 μM) + DNA + H_2O_2; lane 2, $[Co(H_4L)(X)_2]$ (100 μM) + DNA + H_2O_2; lane 3, $[Co(H_4L)(X)_2]$ (75 μM) + DNA + H_2O_2; lane 4, $[Co(H_4L)(X)_2]$ (50 μM) + DNA + H_2O_2; lane 5, $[Co(H_4L)(X)_2]$ (25 μM) + DNA + H_2O_2; lane 6, DNA control.

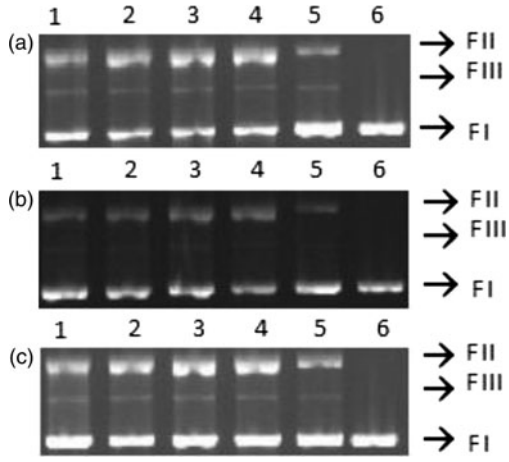

Figure 8. Agarose gel electrophoresis patterns of plasmid pBR 322 DNA after 5 h incubation with various concentrations of complexes **1** (a), **2** (b), **3** (c) in the absence of H_2O_2. Lane 1, $[Co(H_4L)(X)_2]$ (200 μM) + DNA; lane 2, $[Co(H_4L)(X)_2]$ (100 μM) + DNA; lane 3, $[Co(H_4L)(X)_2]$ (75 μM) + DNA; lane 4, $[Co(H_4L)(X)_2]$ (50 μM) + DNA; lane 5, $[Co(H_4L)(X)_2]$ (25 μM) + DNA and lane 6, DNA control.

other titled cobalt(II) complexes may cleavage by an other than oxidative pathway, possibly a hydrolytic pathway.

In the absence of hydrogen peroxide, the cobalt(II) complexes show considerable nuclease activity. When plasmid DNA is incubated for 5 h with the cobalt(II) complex, in the absence of hydrogen peroxide, all three aforementioned complexes convert the supercoiled DNA to Forms II and III but the supercoiled form is still seen (Figure 8(A–C)). The cleavage percentage of nicked form is much higher than that of linear form for all cobalt(II) complexes. On the other hand, in the case of the complex **2**, the cleavage percentages of the form II is much higher than that of form III (Figure 8(B)). It seems that the concentration has a slight effect on DNA cleavage of the titled cobalt(II) complexes in the absence of an oxidative agent.

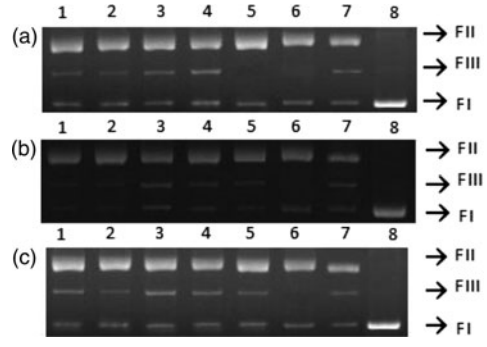

Figure 7. Oxidative plasmid pBR 322 DNA cleavage in the presence of different scavengers and groove binding agents after 3 h incubation with those of the cobalt(II) complexes **1** (a), **2** (b), and **3** (c). Lane 1, $[Co(X)_2(L)]$ + DNA + H_2O_2 + DAPI; lane 2, $[Co(H_4L)(X)_2]$ + DNA + H_2O_2 + methyl green; lane 3, $[Co(H_4L)(X)_2]$ + DNA + H_2O_2 + DMSO; lane 4, $[Co(H_4L)(X)_2]$ + DNA + H_2O_2 + KI; lane 5, $[Co(H_4L)(X)_2]$ + DNA H_2O_2 + NaN_3; lane 6, $[Co(H_4L)(X)_2]$ + DNA + H_2O_2 + catalase; lane 7, $[Co(H_4L)(X)_2]$ + DNA + H_2O_2 + SOD; lane 8, DNA control.

In the absence of an oxidant agent, the DNA cleavage occurs through a hydrolytic pathway, whereas the free diffusible radical species are required for oxidative cleavage of DNA which is inhibited in presence of radical scavengers during the cleavage reaction. It has been also proven that some reactive oxygen species, such as hydroxyl radical, may be produced during the cleavage reactions of metal complexes with DNA, and these radicals may cause the oxidative DNA cleavage. Keeping in mind these facts, the cleavage reactions were also performed with different radical scavengers, such as DMSO, KI, NaN_3, SOD and catalase, in the absence of hydrogen peroxide, to identify the intermediate reactive oxygen species that might be formed in the cleavage reactions. None of these radical scavengers inhibits the DNA cleavage reaction meditated by the titled cobalt(II) complexes (Figure 9). This observation seems to suggest that the DNA cleavages mediated by the titled cobalt(II) complexes are a hydrolytic pathway. On the other hand, it has been also reported that the DNA cleavage mediated by the some copper and zinc complexes occurs via an oxidative mechanism without any oxidising agent (*30*, *49*, *50*). In this situation, the oxidative DNA cleavage can be ligand-based, possibly due to the involvement of a non-diffusible organic radical mechanism that leads to oxidative DNA cleavage. Further studies are undergoing to elucidate the cleavage mechanism.

Supramolecular Chemistry 2015.27:629-641.

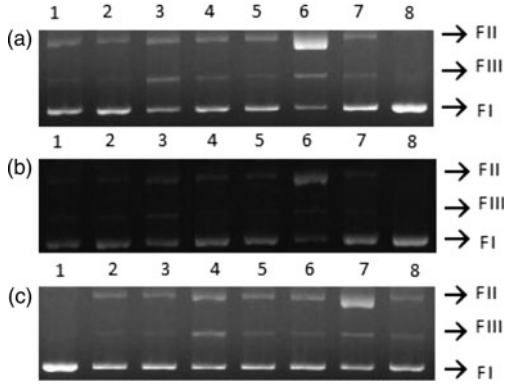

Figure 9. Hydrolytic plasmid pBR 322 DNA cleavage in the presence of different scavengers and groove binding agents after 3 h incubation with of complexes **1** (a), **2** (b) and **3** (c). Lane 1, $[Co(H_4L)(X)_2]$ + DNA + DAPI; lane 2, $[Co(H_4L)(X)_2]$ + DNA + methyl green; lane 3, $[Co(H_4L)(X)_2]$ + DNA + DMSO; lane 4, $[Co(H_4L)(X)_2]$ + DNA + KI; lane 5, $[Co(H_4L)(X)_2]$ + DNA + NaN_3; lane 6, $[Co(H_4L)(X)_2]$ + DNA + catalase; lane 7, $[Co(H_4L)(X)_2]$ + DNA + SOD and lane 8, DNA control.

In order to probe the potential interacting site of the cobalt(II) complexes with plasmid pBR 322 DNA, the effects of groove binding drugs on the strand scission were also determined by using DAPI and methyl green, which are known to bind to DNA at minor groove and major groove, respectively (*51*, *52*). Prior to the addition of the complex, no apparent inhibition of DNA damage is observed in the presence of both DAPI and methyl green (Figures 7 and 9; lanes 1 and 2) neither in presence nor absence of H_2O_2 suggesting that the titled cobalt(II) complexes do not interact with the CT-DNA by groove binding mode.

2.7 Time-dependent DNA cleavage activity

The time course of pBR 322 DNA cleavage mediated by the cobalt(II) complexes (100 μM) was also carried out with agarose gel electrophoresis in the buffer at 37°C in presence and absence of oxidative agent. As shown in Figure 10, in presence of hydrogen peroxide the supercoiled DNA is slightly converted to form II in 0.5 h by the cobalt(II) complexes **1** and **3** (Figure 10(A), lane 7; (C), lane 8). However, the complex **2** cleavages the supercoiled DNA to nicked and linear DNA as soon as it interacts with CT-DNA (Figure 10(B), lane 8). After treatment of the complex with plasmid DNA for 3 h, three forms of DNA are observed indicating that that the cobalt(II) complexes are capable of performing double-strand DNA cleavage after 3 h incubation. When the incubation time increases, the intensity of circular supercoiled form decreases while those of Forms II and III increase gradually. In the case of the complex **1**, Form I almost disappeared after 6 h of incubation (Figure 10(A), lane 1).

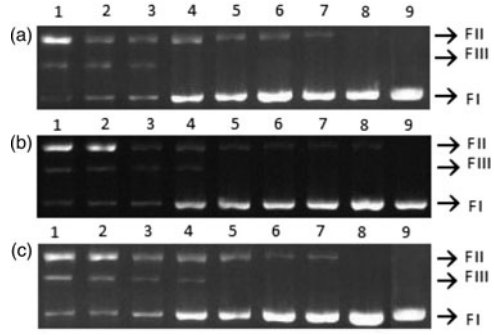

Figure 10. Reaction time dependence of the oxidative DNA cleavage of the cobalt(II) complexes **1** (a), **2** (b) and **3** (c). $[Co(H_4L)(X)_2] = 100\,\mu M$, lane 9: DNA control. The reaction time for lane 1 is 6, 5, 4, 3, 2, 1, 0.5 and 0 h, respectively.

In the absence of any oxidative agent, the cobalt(II) complexes slightly convert the supercoiled DNA into form II in 1 h (Figure 11(A)–(C), lane 7). After treatment of DNA with the cobalt(II) complexes for 2 h, form III also starts to appear slightly besides form II (Figure 11(A)–(C), lane 6). It is also clearly seen that as the incubation time increases, the cleavage intensities of both form II and III increase. The cleavage percentages of form II are much higher than those of form I and III after 6 h DNA interaction.

3. Conclusions

This work reports the synthesis, characterisation and DNA binding and cleavage studies of three seven-coordinated cobalt(II) complexes. The X-ray analyses have revealed a distorted pentagonal–bipyramidal geometry for the cobalt (II) complex. The equatorial plane of the bipyramid is occupied by the pentadentate N_3O_2 2,6-diacetylpyrdine bis (4-hydroxybenzoylhydrazone) ligand while monodentate two NCS^-, N_3^- or H_2O groups occupy the axial position of the complex. UV–vis studies have shown that the titled cobalt(II) complexes seem to bind with CT-DNA through

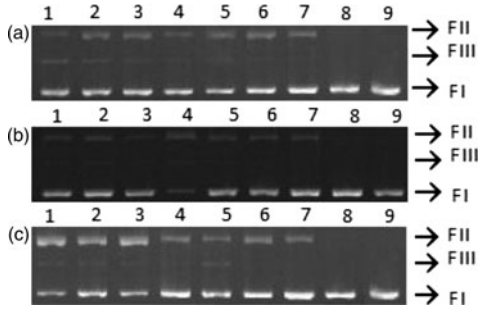

Figure 11. Reaction time dependence of the hydrolytic DNA cleavage by the complexes **1** (a), **2** (b) and **3** (c). $[Co(H_4L)(X)_2] = 100\,\mu M$, lane 9 DNA control. The reaction time for lane 1 is 6, 5, 4, 3, 2, 1, 0.5 and 0 h, respectively.

Supramolecular Chemistry 2015.27:629-641.

covalent binding since the electronic absorption spectra of the cobalt(II) complexes significantly changed upon addition of DNA, indicating that the modification of the architectures of the titled cobalt(II) complexes occurs during DNA interaction. Furthermore, the binding mode of the cobalt(II) complexes is not only covalent binding but also intercalation according to viscosity measurements. The cobalt(II) complexes are able to cleavage DNA both in the presence and absence of oxidant agent. The cleavage of double-stranded DNA by the cobalt(II) complexes has strong dependence on the reaction time as well as the concentration of complex. The various radical scavengers do not effectively inhibit the DNA cleavage mediated by the Co(II) complexes either in the presence or absence of H_2O_2, suggesting that the diffusible radicals are not produced during the DNA cleavage by the cobalt(II) complexes according to the mechanistic studies. These observations seem to suggest that the cobalt(II) complexes cleavage the DNA by an other than oxidative pathway, possible a hydrolytic pathway. However, further studies warrant elucidating the detailed mechanisms of the Co(II) complex-mediated DNA hydrolysis. This study may provide a new approach in the design of more effective and useful seven-coordinated transition metal complexes for DNA binding and cleavage.

4. Experimental

4.1 Material and methods

All the reagents and solvents were of reagent grade quality and were purchased from commercial suppliers. 4-Hydroxybenzohydrazide was synthesised by refluxing ethyl 4-hydroxybenzoate with excess hydrazine hydrate. Calf thymus DNA (CT-DNA) was purchased from Sigma-Aldrich. pBR 322 DNA was purchased from Fermantas. ^{1}H and ^{13}C NMR spectra were recorded on a Bruker 400 MHz spectrometer in DMSO-d_6 with TMS as the internal standard. IR spectra were recorded on pure solid samples with a Thermo-Scientific, Nicolet iS10-ATR (Madison, WI, USA). The electronic spectra of the ligands and complexes were recorded on a PG Instruments T80 + UV/Vis Spectrophotometer (Leicestershire, United Kingdom). Carbon, hydrogen and nitrogen analyses were carried out on a LECO 932 CHNS analyser (Michigan, USA) and cobalt content was determined by atomic absorption spectroscopy using the DV 2000 Perkin Elber ICP-AES (Boston, MA, USA). Room temperature magnetic susceptibility measurements were carried out on powdered samples using a Sherwood Scientific MK1 Model Gouy Magnetic Susceptibility Balance. The thermogravimetric analysis was carried out in dynamic nitrogen atmosphere (20 mL min^{-1}) with a heating rate of 20°C min^{-1} using a Perkin Elmer Pyris TGA 4000 thermal analyser (Boston, MA, USA).

The preparation of 2,6-diacetylpyridine bis(4-hydroxybenzoylhydrazone (H_4L) has been described previously (*53*). Yield: 87%; m.p.: 247–250°C; FT-IR (KBr, cm^{-1}) 3131 b (O—H), 2971 w (CH_3), 1666 m (C═O), 1607 m (C═N), 1263 s (C—O). ^{1}H NMR (DMSO-d_6, ppm) δ 2.52 (s, 6H, C*H*$_3$), 6.87 (d, 4H, Ar*H*) 7.83 (d, 2H, Ar*H*), 8.10 (m, 3H, Py-*H*), 10.16 (s, 2H, OH), 10.66 (s, 2H, NH); ^{13}C NMR (DMSO-d_6, ppm) 180.1 (C═O), 161.3 (C–O), 154.9 (C═N), 137.7, 131.1, 128.3, 124.9, 120.9, and 115.5 (Ar-C), 11.6 (CH_3).

4.2 Synthesis of Co(II) complexes

4.2.1 Synthesis of [Co(H_2L)(H_2O)$_2$] (1)

A solution of $(CH_3COO)_2Co{\cdot}4H_2O$ (0.249 g, 1 mmol) in MeOH (10 mL) was added by dropwise to suspension of the ligand (0.431 g, 1 mmol) in 50 mL MeOH. The reaction mixture was refluxed for 2 h. The precipitated light brown complex was filtered off, and washed with water and methanol. Yield: 85%; m.p.: >350°C. μ_{eff} = 4.24 B.M.; UV (DMF, nm) 268.0, 352.0, 432.0; FT-IR (ATR, cm^{-1}) 3182 b (O—H), 1590 m (C═N—N═C), 1276 s (C—O). MS (ES$^+$), (*m*/*z*): 602.76 [M] $^+$. Analysis (%calculated/found) for $C_{23}H_{23}CoN_5O_6$ C: 52.68/52.90, H: 4.42/4.55, N: 13.36/12.99, Co: 11.25/11.41.

4.2.2 Synthesis of [Co(H_4L)X_2] {X = N_3^- (2) or NCS^- (3)}

A solution of $(CH_3COO)_2Co{\cdot}4H_2O$ (0.249 g, 1 mmol) in MeOH (10 mL) was added dropwise to suspension of the ligand (0.431 g, 1 mmol) in 50 mL MeOH. After the mixture was refluxed for 0.5 h, an aqueous solution of KSCN (0.194 g, 2 mmol in 5 mL) or NaN_3 (0.130 g, 2 mmol) was added, and the resulting mixture was refluxed for further 3 h. The precipitate was filtered off, washed with methanol and diethyl ether several times, and dried in vacuum. The crystals of **3** suitable for X-ray diffraction were obtained upon diffusion of the ethyl ether into the DMF solution.

For [Co(H_4L)(N_3)$_2$] (**2**): Red complex; yield: 83%; m.p.: >350°C. μ_{eff} = 4.27 B.M.; UV (DMF, nm) 268.0, 352.0, 432.0; FT-IR (ATR, cm^{-1}) 3370 b (O–H), 2042 and 1277 s (N═N═N), 1649 m (C═O), 1598 m (C═N), 1238 s (C—O). Analysis (%calculated/found) for $C_{23}H_{21}CoN_{11}O_4$ C: 48.09/47.82, H: 3.68/3.85, N: 26.82/27.10, Co: 10.27/10.85.

For [Co(H_4L)(NCS)$_2$] (**3**): Red complex; yield: 80%; m.p.: >350°C. μ_{eff} = 4.25 B.M.; UV (DMF, nm) 268.0, 354.0, 426.0; FT-IR (ATR, cm^{-1}) 3330 b (O—H), 2089 and 920 s (S═C═N), 1645 m (C═O), 1590 (C═N), 1244 s C—O). Analysis (%calculated/found) for $C_{25}H_{21}CoN_7O_4S_2$ C: 49.50/49.81, H: 3.49/3.25, N: 16.16/16.32, Co: 9.73/9.80.

Supramolecular Chemistry 2015.27:629-641.

4.3 X-ray diffraction study

Crystallographic data were recorded on a Bruker Smart Breeze CCD area-detector diffractometer using MoK_α radiation ($\lambda = 0.71073$ Å) at $T = 296$ (2) K (54). Absorption corrections by multi-scan were applied (55). Cell refinement was carried out using Bruker SAINT and data were reduced by using Bruker SAINT (54). The structure was solved using SHELXS97 and refined using SHELXL2013 (56) by full-matrix least-squares on F^2 against ALL reflections. The weighted *R*-factor *wR* and goodness of fit *S* are based on F^2. The threshold expression of $F^2 > 2\sigma(F^2)$ is used only for calculating *R*-factors. All estimated standard deviations (e.s.d.) are calculated using the full covariance matrix. The cell e.s.d. are taken into account individually in the estimation of e.s.d. in distances, angles and torsion angles; correlations between e.s.d. in cell parameters are only used when they are defined by crystal symmetry. Molecular graphics were drawn ORTEP-3 (57), PLATON (58) and the material for publication prepared using WinGX (59). All non-hydrogen atoms were refined anisotropically and hydrogen atoms were added according to the theoretical model. The fractional atomic coordinates are given in Table S2, supporting information.

4.4 DNA binding

4.4.1 Absorption spectral titrations

Absorption spectral titration experiments involving the interaction of the complexes with CT-DNA were carried out in water buffer containing 5 mM tris [tris(hydroxymethyl)aminomethane] and 50 mM NaCl, and adjusted to pH 7.3 with HCl. The solution of CT-DNA in the buffer gave a ratio of UV absorbance of 1.8 − 1.9:1 at 260 and 280 nm, indicating that the CT-DNA was sufficiently free of protein (60). The CT-DNA concentration per nucleotide was determined spectrophotometrically by employing an extinction coefficient of 6600 $M^{-1}\,cm^{-1}$ at 260 nm (61). An appropriate amount of the cobalt complex was dissolved in a solvent mixture of 1% DMF and 99% tris–HCl buffer. Absorption titration experiments were performed by maintaining the metal complex concentration as constant while gradually increasing the concentration of the CT-DNA within 0–100 μM.

4.4.2 Viscosity measurements

Viscosity experiments were carried out using an Ubbelodhe viscometer at room temperature. The viscosity of CT-DNA solution (25 μM) was measured in the absence and presence of increasing amounts of the complex (6.25–50 μM) in tris–HCl buffer (10 mM tris–HCl–NaCl; pH = 7.6) containing 5% DMF solution. Flow time was measured three times with a digital stopwatch. Viscosity values were presented as $(\eta/\eta_0)^{1/3}$ versus concentrations of [complex]/[DNA] (62) where η was the viscosity value for DNA in the presence of the cobalt(II) complex and η_0 was the viscosity value of CT-DNA alone.

4.5 Chemical nuclease activity

pBR 322 plasmid DNA was used for all cleavage activities. In a typical experiment, 2 μL plasmid DNA (0.50 μg/μL) was mixed with different concentrations of the cobalt(II) complex (25, 50, 75, 100 and 200 μM) dissolved in DMF to determine optimum activation concentration. In the case of oxidative cleavage, 5 μL H_2O_2 (5 mM) was added to the mixture to oxidise the reactant. Finally, the reaction mixture was diluted with the Tris buffer (100 mM Tris, pH: 8) to a total volume of 30 μL. After that reaction, mixtures were incubated at 37°C. Samples (20 μL) were then loaded with 4 μL loading dye (0.25% bromophenol blue, 0.25% xylene cyanol, 30% glycerol, 10 mmol EDTA) on a 1% agarose gel containing 1 μg/mL of EtBr. The gel was run at 100 V for 3 h in TBE buffer and photographed under UV light. To test for the presence of reactive oxygen species generated during strand scission, reactive oxygen intermediate scavengers, that is, SOD, catalase, DMSO, KI and NaN_3 were added alternately to the reaction mixture and the samples were treated as described earlier.

Supporting Information

CCDC 1024060 contains the supplementary crystallographic data for complex *3*. These data can be obtained free of charge via http://www.ccdc.com.

Disclosure statement

No potential conflict of interest was reported by the authors.

Funding

This work was funded by the Scientific and Technological Research Council of Turkey [TÜBİTAK, TBAG-112T315].

References

(1) Erkkila, K.E.; Odom, D.T.; Barton, J.K. *Chem. Rev.* **1999**, *99*, 2777–2796.
(2) Barton, J.K.; Raphael, A.L. *J. Am. Chem. Soc.* **1984**, *106*, 2466–2468.
(3) Ramakrishnan, S.; Suresh, E.; Riyasdeen, A.; Akbarsha, M.A.; Palaniandavar, M. *Dalton Trans.* **2011**, *40*, 3245.
(4) Lahiri, D.; Roy, S.; Saha, S.; Majumdar, R.; Dighe, R.R.; Chakravarty, A.R. *Dalton Trans.* **2010**, *39*, 1807.
(5) Thyagarajan, S.; Murthy, N.N.; Sarjeant, A.A.N.; Karlin, K.D.; Rokita, S.E. *J. Am. Chem. Soc.* **2006**, *128*, 7003–7008.
(6) Gup, R.; Gökçe, C.; Dilek, N. *J. Photochem. Photobiol. B* **2015**, *144*, 42–50.

(7) Ahmad, M.; Afzal, M.; Tabassum, S.; Kalinska, B.; Mrozinski, J.; Bharadwaj, P.K.; Eur *J. Med. Chem.* **2014**, *74*, 683–693.
(8) Indumsthy, *R.*; Kanthimathi, M.; Weyherrmuller, T.; Nair, B.U. *Polyhedron* **2008**, *27*, 3443–3450.
(9) Eshkourfu, R.; Cobeljic, B.; Vujcic, M.; Turel, I.; Pevec, A.; Sepcic, K.; Zec, M.; Radulovic, S.; Srdic-Radic, T.; Mitic, D.; Andjelkovic, K.; Sladic, D. *J. Inorg. Biochem.* **2011**, *105*, 1196–1203.
(10) Selvi, P.T.; Stoeckli-Evans, H.; Palaniandavar, M. *J. Inorg. Biochem.* **2005**, *99*, 2110–2118.
(11) Hall, M.D.; Failes, T.W.; Yamamoto, N.; Hambley, T.W. *Dalton Trans.* **2007**, *36*, 3983–3990.
(12) Lopez-Sandoval, H.; Londono-Lemos, M.E.; Garza-Velasco, R.; Poblano-Melendez, I.; Granada-Macias, P.; Gracia-Mora, I.; Barba-Behrens, N. *J. Inorg. Biochem.* **2008**, *102*, 1267–1276.
(13) Ott, I.; Abraham, A.; Schumacher, P.; Shorafa, H.; Gasti, G.; Gust, R.; Kircher, B. *J. Inorg. Biochem.* **2006**, *100*, 1903–1906.
(14) Miodragovic, D.U.; Bogdanovic, G.A.; Miodragovic, Z.M.; Radulovic, M.D.; Novakovic, S.B.; Kaluderovic, G.N.; Kozłowski, H. *J. Inorg. Biochem.* **2006**, *100*, 1568–1574.
(15) Nomiya, K.; Yoshizawa, A.; Tsukagoshi, K.; Kasuga, N.C.; Hirakawa, S.; Watanabe, J *J. Inorg. Biochem.* **2004**, *98*, 46–60.
(16) Lv, J.; Liu, T.; Cai, S.; Wang, X.; Liu, L.; Wang, Y. *J. Inorg. Biochem.* **2006**, *100*, 1888–1896.
(17) Weiqun, Z.; Wen, Y.; Liqun, X.; Xianchen, C. *J. Inorg. Biochem.* **2005**, *99*, 1314–1319.
(18) Bottcher, A.; Takeuchi, T.; Hardcastle, K.I.; Meade, T.J.; Gray, H.B. *Inorg. Chem.* **1997**, *36*, 2498–2504.
(19) Takeuchi, T.; Bottcher, A.; Quezada, C.M.; Meade, T.J.; Gray, H.B. *Bioorg. Med. Chem.* **1999**, *7*, 815–819.
(20) Dimiza, F.; Papadopoulos, A.N.; Tangoulis, V. *Dalton Trans.* **2010**, *39*, 4517–4528.
(21) Tsilou, S.; Kefala, L.A.; Perdih, F.; Turel, I.; Kesisoglou, D.P.; Psomas, G. *Eur. J. Med. Chem.* **2012**, *142*, 48–132.
(22) Dimiza, F.; Papadopoulos, A.N.; Tangoulis, V.; Psycharis, V.; Raptopoulou, C.P.; Kesisoglou, D.P.; Psomas, G. *J. Inorg. Biochem.* **2012**, *107*, 54–64.
(23) Dimiza, F.; Papadopoulos, A.N.; Tangoulis, V.; Psycharis, V.; Raptopoulou, C.P.; Kesisoglou, D.P.; Psomas, G. *Dalton Trans.* **2010**, *39*, 4517–4528.
(24) Carcelli, M.; Mazza, P.; Pellizzi, G.; Zani, F. *J. Inorg. Biochem.* **1995**, *57*, 43–62.
(25) Gökçe, C.; Dilek, N.; Gup, R. *Inorg. Chim. Acta* **2015**, *432*, 213–220.
(26) Ferraz, K.S.O.; Silva, N.F.; da Silva, J.G.; de Miranda, L.F.; Romeiro, C.F.D.; Souza-Fagundes, E.M.; Mendes, I.C.; Beraldo, H. *Eur. Med. Chem.* **2012**, *53*, 98–106.
(27) Bottari, B.; Maccari, R.; Monforte, F.; Ottana, R.; Vigorita, M.G.; Bruno, G.; Nicola, F.; Rotondo, A.; Rotondo, E. *Biorg. Med. Chem.* **2001**, *9*, 2203–2211.
(28) Ivanovic-Burmazovic, I.; Bacchi, A.; Pelizzi, G.; Leovac, V.M.; Andjelkovic, K. *Polyhedron* **1999**, *18*, 119–127.
(29) Kozlowski, M.; Kierzek, R.; Kubicki, M.; Radecka-Paryzek, W. *J. Inorg. Biochem.* **2013**, *126*, 38–45.
(30) Gokce, C.; Gup, R. *Photochem. Photobiol. B* **2013**, *122*, 15–23.
(31) Gokce, C.; Gup, R. Appl. Organomet. Chem. **2013**, *27*, 263–268.
(32) Gup, R.; Kırkan, B. *Spectrochim. Acta A* **2006**, *64*, 809–815.
(33) Li, M.J.; Lan, T.Y.; Lin, Z.S.; Yi, C.; Chen, G.N. *J. Biol. Inorg. Chem.* **2013**, *18*, 993–1003.
(34) Lorenzini, C.; Pelizzi, C.; Pelizzi, G.; Predieri, G. *J. Chem. Soc. Dalton Trans.* **1983**, *4*, 721–727.
(35) Jesic, L.S.V.; Cesljevic, V.I.; Bogdanovic, G.A.; Leovac, V.M.; Szecsenyi, K.M.; Divjakovic, V.; Joksovic, M.D. *Inorg. Chem. Commun.* **2010**, *13*, 1085–1088.
(36) Gup, R.; Giziroglu, E.; Kırkan, B. *Dyes Pigments* **2007**, *73*, 40–46.
(37) Renaud, R.; Batchelor, L.J.; Maurice, R.; Gogoi, N.; Lozano, P.J.; Guihery, N.; de Graaf, C.; Barra, A.L.; Sutter, J.P.; Mallah, T. *Chem. A Eur. J.* **2013**, *19*, 950–956.
(38) Giordano, T.J.; Palenik, G.J.; Palenik, R.C.; Sullivan, D.A. *Inorg. Chem.* **1979**, *18*, 2445–2450.
(39) Barton, J.K.; Danishhefsky, A.T.; Goldberg, J.M. *J. Am. Chem. Soc.* **1984**, *106*, 2172–2176.
(40) Hirohama, T.; Kuranuki, Y.; Ebina, E.; Sugizaki, T.; Arii, H.; Chikira, M.; Selvi, P.T.; Palaniandavar, M. *J. Inorg. Biochem.* **2005**, *99*, 1205–1219.
(41) Barton, J.K.; Dannenberg, J.J.; Raphael, A.L.J. *Am. Chem. Soc.* **1982**, *104*, 4967–4969.
(42) Ghosh, K.; Kumar, P.; Tyagi, N. *Inorg. Chim. Acta* **2011**, *375*, 77–83.
(43) Raja, A.; Rajendiran, V.; Maheswari, P.U.; Balamurugan, R.; Kilner, C.A.; Halcrow, M.A.; Palaniandavar, M. *J. Inorg. Biochem.* **2005**, *99*, 1717–1732.
(44) Icsel, C.; Yilmaz, V.T.; Golcu, A.; Ulukaya, E.; Buyukgungor, O. *Bioorg. Med. Chem. Let.* **2013**, *23*, 2117–2122.
(45) Satyanarayana, S.; Dabrowiak, J.C.; Chaires, J.B. *Biochemistry* **1992**, *31*, 9319–9324.
(46) Quinn, J.P.; McGeoch, D.J. *Nucleic Acids Res.* **1985**, *13*, 8143–8163.
(47) Reinert, K.E. *Biophys. Chem.* **1981**, *13*, 1–14.
(48) Massoud, S.S.; Louka, F.R.; Xu, W.; Perkins, R.S.; Vicente, R.; Albering, J.H.; Mautner, F.A.; *Eur J. Inorg. Chem.* **2011**, *23*, 3469–3479.
(49) Garrido, N.J.; Perello, L.; Ortiz, R. *J. Inorg. Biochem.* **2005**, *99*, 677–689.
(50) Gup, R.; Gökçe, C.; Aktürk, S. *Spectrochim. Acta Part A* **2015**, *134*, 484–492.
(51) Trotta, E.; Grosso, N.D.; Erba, ;.M.; Paci, M. *Biochemistry* **2000**, *39*, 6799–6808.
(52) Dong, X.; Wang, X.; Lin, M.; Sun, H.; Yang, X.; Guo, Z. *Inorg. Chem.* **2010**, *49*, 2541–2549.
(53) Dilek, N.; Güneş, B.; Büyükgüngör, O.; Gup, R. *Crystallogr. Rep+* **2013**, *58*, 98–101.
(54) Bruker, *Bruker, APEX2, SAINT and SADABS*; Bruker AXS: Madison, WI, 2005.
(55) Blessing, R.H. *Acta Crystallogr.* **1995**, *A51*, 33–38.
(56) Sheldrick, G.M *Acta Crystallogr.* **2008**, *A64*, 112–122.
(57) Farrugia, L.J. *Appl. Crystallogr.* **1997**, *30*, 565.
(58) Spek, A.L. *PLATON: Multipurpose Crystallographic Tool*; Utrech University, Netherlands, 1998.
(59) Farrugia, L.J. *Appl. Crystallogr.* **1999**, *32*, 837–838.
(60) Marmur, J. *J. Mol. Biol.* **1961**, *3*, 208–218.
(61) Pyle, A.M.; Rehmann, J.P.; Meshoyrer, J.P.; Kumar, C.V.; Turro, N.J.; Barton, J.K. *Am. Chem. Soc.* **1989**, *111*, 3053–3058.
(62) Cohen, G.; Eisenberg, H. *Biopolymers* **1969**, *8*, 45–55.

Supramolecular Chemistry 2015.27:629-641.